VU limit pre-assessment for high-speed railway considering a grid connection scheme

Chen, Yinyu; Chen, Minwu; Tian, Zhongbei; Liu, Yuanli; Hillmansen, Stuart

DOI:
10.1049/iet-gtd.2018.6323

Voltage unbalance limit pre-assessment for high-speed railway considering a grid connection scheme

Yinyu Chen [1], Minwu Chen [1*], Zhongbei Tian [2], Yuanli Liu [1], Stuart Hillmansen [2]

[1] School of Electrical Engineering, Southwest Jiaotong University, Chengdu, People's Republic of China
[2] Birmingham Centre for Railway Research and Education, School of Engineering, University of Birmingham, Birmingham, UK
[*]chenminwu@home.swjtu.edu.cn

Abstract: Single-phase 25-kV AC traction power supply systems (TPSSs) are widely used in high-speed railways (HSRs), leading to an increasingly prominent problem of voltage unbalance (VU) in the power grid. To fairly regulate the system VU level, implementing VU limit pre-assessment is an urgent need. A grid connection scheme, including traction transformer selection and exchange phase connection (EPC) design, is a vital part of TPSS design that obviously affects the voltage unbalance factor (VUF) of power systems. A uniform mathematical model is established using Thevenin's theorem, which reveals the impact of multiple grid connection schemes on the VU propagation behaviour of a three-phase grid. Afterwards, under the requirements of IEC/TR 61000-3-13, an improved VU limit pre-assessment process is proposed, which correlates mapping between the grid connection scheme and VU limit. The unbalance compensation calculation is given, adopting the allocation limit; furthermore, the optimal design of the grid connection scheme with minimized compensation capacity as an object is presented. The correctness of the model and the rationality of the pre-assessment process are verified by a case study.

Nomenclature

ψ_α, ψ_β	transformer phase angle of α and β feeding sections, respectively
k_T	ratio of the port voltage of the transformer traction side and the phase voltage of the transformer primary side
$\dot{I}_{\alpha\beta}, \dot{U}_{\alpha\beta}$	current and voltage matrices of the feeding section, respectively
$\varphi_\alpha, \varphi_\beta$	power factor of α and β feeding sections, respectively
$\dot{E}_{\alpha\beta}$	two-phase voltage matrix of a TSS
$Z_{\alpha\beta}$	leakage reactance matrix
$\dot{E}_{trac}^{abc}$	three-phase voltage matrix of a TSS
Z_{line}^{++}	positive sequence implement
Z_{line}^{--}	negative sequence implement
Z_{line}^{+-}	coupling implement between positive and negative sequences
$\dot{k}_{i:x}$	influence coefficient
$S_{dc:x}$	short-circuit capacity of bus x
$S_{x:j}$	apparent power of customer installation j at bus x
$\dot{U}_{x:U_i}$	negative sequence voltage at busbar x which propagates from busbar i
$\dot{I}_{line:U_i}^{-}$	negative sequence current in the transmission line arising from unbalance at the busbar i
$C_{x:i}$	contribution coefficient
$E_{x:j}$	customer emission limit
α	summation law exponent
$U_{g:x}$	bus planning level
$S_{tot:x}$	total supply capacity of the system considered including provision for future load growth and contribution from other buses
s_{comp}^{-}	compensator capacity
S_{Σ}^{-}	negative sequence capacity that can make the VUF of bus x meet the VU limit pre-assessment
S_1^+	positive apparent power
S_{u1}	unbalance apparent power

1. Introduction

Due to the growing construction of high-speed railways (HSRs), power quality problems caused by single-phase 25-kV AC traction power supply systems (TPSSs) have attracted more and more attention. The voltage unbalance (VU) problem has been a severe issue in practical engineering throughout Europe and China [1–4]. It causes serious grid operation accidents in areas with a vulnerable grid structure [5–7], especially in mid-western China. For example, Sanmenxia wind farm was cut off due to the operation of the Zhengzhou-Xi'an HSR [8, 9]. As shown in Fig. 1, the grid connection scheme is an essential part of TPSS design. In the area in which the VU distribution and VU limit pre-assessment of traction substation (TSS), choosing a reasonable scheme plays an important role [4], especially for exchange phase connection (EPC) scheme design and special three-phase to one-phase traction transformer selection.

The study of VU propagation is presented in the literature [10–12], covering radical and interconnected networks. This method depends strictly on equivalent circuits and considering all unbalanced sources (including the upstream source, transmission line and unbalanced ZIP load). However, the TPSS cannot be simplified as a ZIP model because the special traction transformer cannot be equivalent to a general transformer in the power grid. On the other hand, the model presented focuses mainly on a three-phase unbalanced source, as a uniform model between three-phase and single-phase has not been established; Jayatunga *et al.* [11, 12] established a model to consider multiple unbalanced loads such as inductive motor and ZIP loads; Sun *et al.* [13] built a propagation model to portray multiple three-phase asymmetric sources; Mahyar *et al.* [14] presented a new method to determine the contribution of different effective factors in an n-bus radial distribution system; Sun *et al.* [15] proposed a method to identify the main unbalanced source at

the point of evaluation in the distribution power systems; He *et al.* [16] have proposed an approximation algorithm for fast calculation of voltage unbalances in three-phase power systems; Perera *et al.* [17] have presented a detailed analysis of VU attenuation and propagation in radial distribution lines and proposed a methodologies for estimating the VU transfer coefficients. More importantly, the impact of multiple grid connection schemes on the VU propagation behaviour of three-phase grids needs to be studied. Thus, there is an urgent demand to establish a uniform VU propagation model.

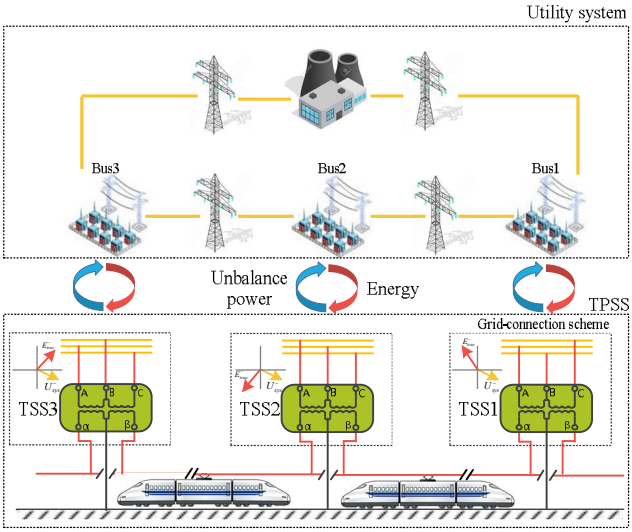

Fig. 1. *Description of China's HSR system*

Alternatively, the total voltage unbalance factor (VUF) result at the bus is not solely responsible for the unbalanced load; it is also influenced by surrounding unbalance which is transferred through the neighbouring bus [10]. To ensure that the VUF at the bus meets the requirements of the standard, how the power grid fairly regulates various unbalanced sources is a severe challenge, especially in regions with a weak power grid structure. In mid-western and north-western China, for example, the short-circuit capacity of the bus is less than 2000 MVA; to meet the requirements of GB/T 15543 [18], the capacity of the TSS should not exceed 1.3%×2000=26 MVA. Nonetheless, the rated power of a traction transformer is up to 100 MVA in TSSs. Therefore, there is a pressing need to establish a flexible VU limit pre-assessment process, particularly considering the effect of the grid connection scheme. The IEC/TR 61000-3-13 guideline provides a new way to manage VU in power grids [19]. The three-stage pre-assessment process is one of the most important achievements of this report. In this regard, there are a lot of contributions that apply the report to power grids [20–22]. In addition, the United Kingdom, Australia, Denmark, etc., have formulated and published VU management standards based on IEC/TR 61000-3-13 [23–25]. Unfortunately, previous works have lacked an important discussion on how to modify the pre-assessment process to consider the impact of the grid connection scheme.

In this paper, a port transformation model of a TSS is described in section 2. A uniform mathematical model of VU propagation, considering the influence of the grid connection scheme, has been established in section 3. In section 4, a VU limit pre-assessment process in terms of a grid connection scheme has been proposed. In section 5, the unbalanced compensation calculation is presented. An optimal design for a grid connection scheme is proposed, to minimize the accumulated compensator capacity. In section 6, a typical circle-wise power system is used to verify the model and approach above.

2. TSS port transformation model

2.1. Port transformation matrix

The topology model of a TSS is shown in Fig. 2. $\dot{U}_\alpha(\dot{U}_\beta)$ and $\dot{I}_\alpha(\dot{I}_\beta)$ are the voltage and current of the traction side, respectively. $\dot{E}_{abc}$ and $\dot{I}_{abc}$ are the voltage and current of the grid side, respectively. V/v and Scott traction transformers are widely used for HSRs around the world.

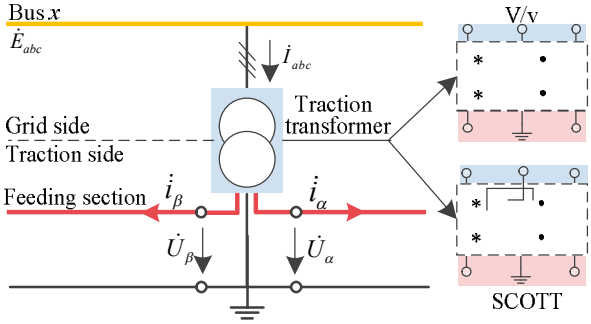

Fig. 2. *TSS topology model*

According to the power conservation theorem of a traction transformer,

$$\underbrace{\dot{U}_{abc}\dot{I}^*_{abc}}_{\text{Grid side}} = \underbrace{\sum_{i=1}^{2}\dot{U}_i\dot{I}^*_i = \sum_{i=1}^{2}U_i e^{-j\psi_i}\dot{I}^*_i}_{\text{Traction side}} \tag{1}$$

where i is a port on the traction side, such as port α or β in this paper, and ψ_i is the traction transformer phase angle (the value is given in *Appendix A*), defined as the angle between the positive voltage of the grid side and the port voltage of the traction side:

$$\psi_i = \angle\left(U^+_{abc} \quad U_i\right) \tag{2}$$

Under the effect of positive and negative voltage, the relationship of the current on the grid and traction sides is expressed as:

$$\dot{I}_{abc} = \begin{pmatrix}1 & 1 & 1\\ 1 & a^2 & a\\ 1 & a & a^2\end{pmatrix}^{-1}\begin{pmatrix}0\\ \sqrt{3}k_T e^{j\psi_i}\\ \sqrt{3}k_T e^{-j\psi_i}\end{pmatrix}\sum_{i=1}^{2}\dot{I}_i = T^{-1}D\sum_{i=1}^{2}\dot{I}_i \tag{3}$$

where $a = e^{j2\pi/3}$, and k_T is the ratio of the port voltage of the transformer traction side and the phase voltage of the transformer primary side.

Thus, the current transformation matrix C is defined as (see *Appendix B*):

$$C = T^{-1}D = \frac{2}{\sqrt{3}}\begin{bmatrix}K_\alpha\cos\psi_\alpha & K_\beta\cos\psi_\beta\\ K_\alpha\cos\left(120^\circ-\psi_\alpha\right) & K_\beta\cos\left(120^\circ-\psi_\beta\right)\\ K_\alpha\cos\left(120^\circ+\psi_\alpha\right) & K_\beta\cos\left(120^\circ+\psi_\beta\right)\end{bmatrix} \tag{4}$$

At the same time, the voltage transformation matrix V is defined as:

$$V = C^T \tag{5}$$

Different grid connection schemes have different transformation matrices (see *Appendix A*). For a V/v traction transformer, $\Psi_\beta = \Psi_\alpha + 120°, K_\alpha = K_\beta = k_T$. For a Scott traction transformer, $\Psi_\beta = \Psi_\alpha \pm 90°, K_\alpha = K_\beta = k_T$.

2.2. Equivalent model of a TSS

According to the Thevenin's theorem, the equivalent two-phase model of a TSS is shown in Fig. 3. The grid side is equivalent to the traction side, and $\dot{E}_{\alpha\beta}$ is equivalent to $\dot{E}_{abc}$.

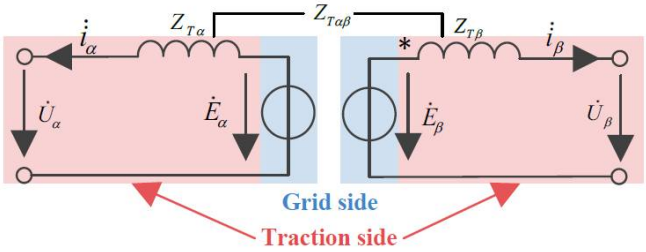

Fig. 3. *Equivalent two-phase model of a TSS*

The two-phase voltage matrix of TSS $\dot{E}_{\alpha\beta}$ can be expressed as:

$$\dot{E}_{\alpha\beta} = Z_{\alpha\beta}\dot{I}_{\alpha\beta} + \dot{U}_{\alpha\beta} \tag{6}$$

where $Z_{\alpha\beta}$ is the leakage reactance matrix and $\dot{U}_{\alpha\beta}$ is the voltage matrix of the feeding section

The equivalent three-phase model of a TSS is shown in Fig. 4; the traction side is equivalent to the grid side.

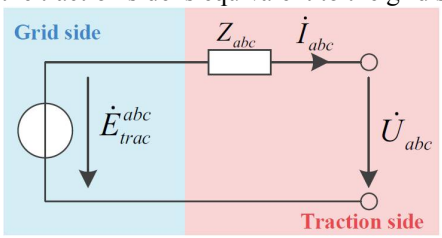

Fig. 4. *Equivalent three-phase model of a TSS*

The three-phase voltage matrix of the TSS $\dot{E}^{abc}_{trac}$ can be expressed as (see *Appendix B*):

$$\begin{aligned}\dot{E}^{abc}_{trac} &= V^{-1}\dot{E}_{\alpha\beta} = V^{-1}Z_{\alpha\beta}C^{-1}\dot{I}_{abc} + V^{-1}\dot{U}_{\alpha\beta} \\ &= Z_{abc}\dot{I}_{abc} + \dot{U}_{abc}\end{aligned} \tag{7}$$

$\dot{E}^{abc}_{trac}$ can be transformed into symmetrical impedances $\dot{E}^{+-}_{trac}$ with matrix T:

$$\dot{E}^{+-}_{trac} = T\dot{E}^{abc}_{trac} = \begin{bmatrix}1 & a & a^2 \\ 1 & a^2 & a\end{bmatrix}\dot{E}^{abc}_{trac} \tag{8}$$

3. Uniform VU propagation model in term of the TPSS and power grid

The topology of a uniform model of a TSS and power grid is shown in Fig. 5. Bus 1…*i*…*n* can be seen as an asymmetric source.

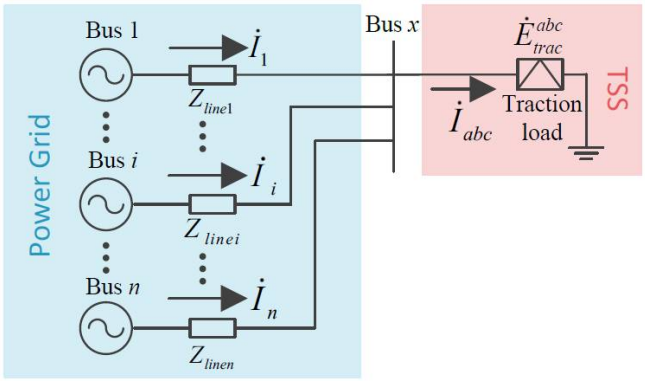

Fig. 5. *Uniform topology model of a TSS and power grid*

When bus i connects to bus x, the voltage sequence component equation at bus x based on KVL can be written as equation (9):

$$\begin{bmatrix}\dot{U}^+_x \\ \dot{U}^-_x\end{bmatrix} = \underbrace{\begin{bmatrix}\dot{U}^+_i \\ \dot{U}^-_i\end{bmatrix} - \begin{bmatrix}Z^{++}_{line:i} & Z^{+-}_{line:i} \\ Z^{+-}_{line:i} & Z^{--}_{line:i}\end{bmatrix}\begin{bmatrix}\dot{I}^+_i \\ \dot{I}^-_i\end{bmatrix}}_{\text{Part I}} - \underbrace{\begin{bmatrix}E^+_{trac} \\ E^-_{trac}\end{bmatrix}}_{\text{Part II}} \tag{9}$$

Equation (9) has two parts: Part I is the surrounding sequence voltage which is transferred through the neighbouring bus i, and Part II is the equivalent three-phase model of a TSS as in equation (8).

When the transmission line is symmetric, the coupling implement between positive and negative sequences (Z^{+-}_{line}) can be ignored. Thus, equation (9) can be rewritten as:

$$\begin{cases}\dot{U}^+_x = \dot{U}^+_i - Z^{++}_{line:i}\dot{I}^+_i - \dot{E}^+_{trac} \\ \dot{U}^-_x = \dot{U}^-_i - Z^{--}_{line:I}\dot{I}^-_i - \dot{E}^-_{trac}\end{cases} \tag{10}$$

The influence coefficient can quantify VU propagation between the different buses [10]. The calculation method in an interconnected network proposed by Jayatunga *et al.* [11, 12, 20] removes the obstacle of calculating VU propagation in a complex network. The influence coefficient $\dot{k}_{i:x}$ is defined as the VU arising at busbar x when 1 pu of negative sequence voltage source is applied at busbar i [19], which can be expressed as:

$$\dot{k}_{i:x} = \frac{\dot{U}_{x:U_i}}{\dot{U}^-_i} = \frac{\dot{U}^-_x - Z^{++}_{line}\dot{I}^-_{line:U_i}}{\dot{U}^-_i} \tag{11}$$

where $\dot{U}_{x:U_i}$ is the negative sequence voltage at busbar x which propagates from busbar i, and $\dot{I}^-_{line:U_i}$ is the negative sequence current in the transmission line arising as a result of the unbalance at busbar i.

It should be noted that the positive sequence impedance of transmission line ($\dot{Z}^{++}_{line}$) is equal to negative sequence impedance ($\dot{Z}^{--}_{line}$) for transmission line. Therefore, the voltage sequence component equation at bus x in terms of the influence coefficient can be written as:

$$\begin{cases}\dot{U}^+_x = \dot{U}^+_i - Z^{++}_{line:i}\dot{I}^+_i - \dot{E}^+_{trac} \\ \dot{U}^-_x = \dot{k}_{i:x}\dot{U}^-_i - \dot{E}^-_{trac}\end{cases} \tag{12}$$

When n buses are connected to bus x, a uniform VU propagation model is established, which can be expressed as:

$$\begin{cases} \dot{U}^{+}_{x:j} = \left(\sum_{i=1}^{n} \dot{U}^{+}_{i} - Z^{++}_{line:i} \dot{I}^{+}_{i} \right) - \dot{E}^{+}_{trac} \\ \dot{U}^{-}_{x:j} = \left(\sum_{i=1}^{n} \dot{k}_{i:x} \dot{U}^{-}_{i} \right) - \dot{E}^{-}_{trac} \end{cases} \quad (13)$$

Equation (13) illustrates the impact of multiple grid connection schemes on the VU propagation behaviour of a three-phase grid. On the other hand, this model can provide a guide to an optimal design grid connection scheme, since the composition of bus VU can be clearly divided by the VU propagation model.

4. VU limit pre-assessment process in terms of grid connection scheme

4.1 Customer emission limit (CEL) allocation method in IEC/TR 61000-3-13

To fairly regulate the system VU level and allocate the CEL of an unbalanced load, IEC/TR 61000-3-13 follows two basic philosophies:

(1) The first rule is consistency, that the VU at any point on the public grid should not exceed the planning level.

(2) The second rule is fairness, that the planning level should be fairly allocated in the public grid. The allocation method should be based on the capacity of load rather than on load type, i.e. equal capacity for different types of load installed on the same bus, and it should have an equal emission limit while high-capacity users have a higher VU limit.

Based on the principle above, the three-stage pre-assessment process is established as:

- Stage 1: If the ratio of the power equivalent of customer j and the grid short-circuit capacity at busbar x satisfies equation (14), customer j can directly connect to the public grid without an emission limit.

$$\frac{S_{x:j}}{S_{dc:x}} \le 0.2\% \quad (14)$$

where $S_{dc:x}$ is the short-circuit capacity of bus x, and $S_{x:j}$ is the apparent power of customer installation j at bus x, which can be defined as:

$$S_{x:j} = \frac{P_{x:j}}{\cos\varphi_{x:j}} \quad (15)$$

- Stage 2: If customer j cannot meet the requirement of stage 1, it should comply with a CEL ($E_{x:j}$). The allocation method is expressed as:

$$E_{x:j} = \sqrt[\alpha]{Kue_x} U_{g:x} \sqrt[\alpha]{\frac{S_{x:j}}{S_{tot:x}}} \quad (16)$$

where $U_{g:x}$ is the bus planning level, Kue_x represents the fraction of $U_{g:x}$ that can be allocated to customer installations, when the transmission line is symmetrical, and $Kue_x = 1$. $S_{tot:x}$ is the total available apparent power of the entire system that considers the VU contributions from adjacent busbars 1, 2, …, n in terms of influence coefficients $k_{i:x}$:

$$S_{tot:x} = k_{1:x} S_1 + k_{2:x} S_2 + \ldots + S_x + \ldots + k_{n:x} S_n \quad (17)$$

Unfortunately, Paranavithana *et al.* [21, 26] have reported that the result of equation (16) renders the actual bus VU level higher than the planning level, even when no VUF of a customer exceeds the CEL. Thus, the constraint bus voltage method is present, which can be expressed as:

$$E_{x:j} = k_a \sqrt[\alpha]{Kue_x S_{x:j}} \quad (18)$$

where k_a is the allocated coefficient, which can be defined as:

$$k_a = \frac{U_{g:x}}{\max\left[\sqrt[\alpha]{S_x + \sum_{i=1}^{n} \left(k^{\alpha}_{i:x} S_i \right)} \right]} \quad (19)$$

- Stage 3: If customer j cannot meet the requirement of stage 2, the customer should consult the operator of the public grid.

Whether the apparent power of customer installation j can be accurately calculated plays a vital role in allocating CEL fairly. However, equation (15) is not accurate enough to calculate the greatest possible apparent power absorbed by an unbalanced load [27, 28], as the apparent power of the coupling effect between positive and negative sequence components should be calculated. More importantly, this partial energy arouses power or torque oscillation in inductive motors [7].

To dispose of this problem, the IEEE-SA released IEEE Std 1459 in 2010 [29] that defines powers with a clear physical significance under non-sinusoidal and asymmetrical power system conditions.

For a three-wire asymmetrical power system, the 'effective' values of voltage (V_e), current (I_e) and apparent power (S_e) are used to quantify the impact on VU in a practical manner [30]. Thus, the apparent power of customer installation j at bus x $S_{x:j}$ is defined as:

$$S_{x:j} = S_e = 3 V_e I_e \quad (20)$$

where

$$\begin{cases} V_e = V_{e1} = \sqrt{\left(V_1^{+}\right)^2 + \left(V_1^{-}\right)^2} \\ I_e = I_{e1} = \sqrt{\left(I_1^{+}\right)^2 + \left(I_1^{-}\right)^2} \end{cases} \quad (21)$$

Furthermore, taking account of positive and negative components, effective apparent power can be expressed as:

$$\begin{aligned} S_e^2 &= S_{e1}^2 = 9 V_{e1}^2 I_{e1}^2 \\ &= 9\left(V_1^{+} I_1^{+}\right)^2 + 9\left[\left(V_1^{+} I_1^{-}\right)^2 + \left(V_1^{-} I_1^{+}\right)^2 + \left(V_1^{-} I_1^{-}\right)^2\right] \\ &= \left(S_1^{+}\right)^2 + \left(S_{u1}\right)^2 \end{aligned} \quad (22)$$

where S_1^{+} and S_{u1} are positive apparent power and unbalanced apparent power at a fundamental frequency, respectively.

4.2 Improved VU limit pre-assessment process

Combining the port transformation model of a TSS, a uniform VU propagation model and a three-stage pre-assessment process, a VU limit pre-assessment process in terms of the grid connection scheme is proposed in Fig. 6; it includes three parts:

(1) Calculating the CEL of TSS j at bus x, based on the port transformation model of a TSS and a uniform VU propagation model. The interrelationship between the grid connection scheme and VU limit is revealed in this part.
(2) Simulating the prospective VUF of TSS ($VUF_{x:j}$) and comparing it with the CEL of the TSS.
(3) If $VUF_{x:j} > E_{x:j}$, which means the prospective VUF is higher than the limit, the railway should install compensation. If $VUF_{x:j} < E_{x:j}$, the VU limit pre-assessment of the TSS is acceptable.

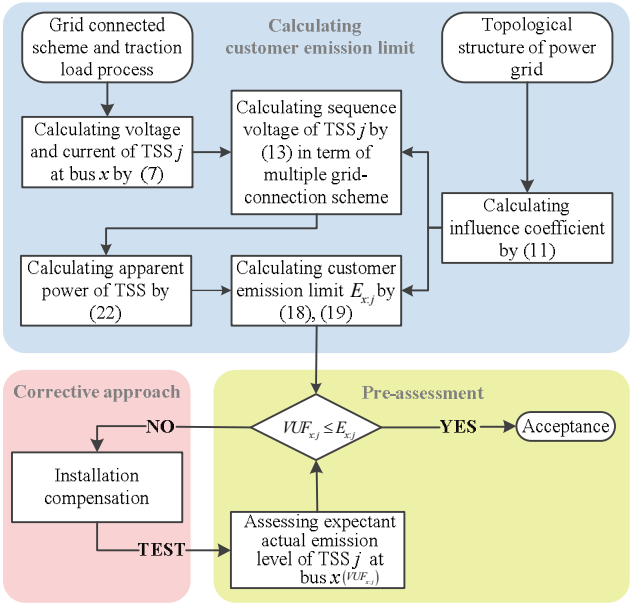

Fig. 6. *Flow chart of the VU limit pre-assessment process*

Nevertheless, to eliminate the VU question, the railway needs to pay the high investment cost of the compensator [1, 2, 4]. How the compensation capacity can be reduced will be illustrated in next section.

5. HSR grid connection scheme optimization

5.1 Converter-based compensation

There are three mainly approaches to eliminate or reduce VU problem for a TPSS.

- The SVC is used widely in railway field during in the past 20 years, which benefits from the simple structure and low cost, but its weakness that effect on series and shunt resonance frequency is increasingly highlighted [2].
- The railway power conditioner (RPC) is proposed in Japan, which there are two back-to-back single- phase converters connected to two feeding sections, it still is the most popular compensation equipment in the field of electrified railway power quality problem at present [31, 32]. Compering the co-phase system, the most prominent advantage is low capacity, as it should not undertake all the power demand of TSS, just compensates the part of power fluctuation. However, it cannot eliminate the neutral zones, thus the availability of regenerative braking energy is apparent less than co-phase system, and it cannot solve the transient overvoltage problems.
- The co-phase system is presented by Li [33] in China, which using a converter to replace the traditional traction transformer. This system not only can eliminate or reduce the power quality problem, but also can eliminate the neutral zones. It has been adopted in Meishan, China [1, 33, 34].

There is a situation should be pointed, the manufacturing cost of convertor is still expensive, especially for a high capacity devices with high voltage level. Thus, many researches have proposed the partial compensating scheme, in which the compensation objective just satisfy the power quality standard [31, 35, 36]. In this regard, an unbalanced compensation calculation method will be illustrated in next section.

5.2 Unbalanced compensation calculation for a TPSS

According to the previous discussion on the traditional power definition and flexible VU limit allocation method, the method presented is inaccurate. Thus, a modified calculation method is proposed in this paper, based on the IEC/TR 61000-3-13 [19] and IEEE Std 1459 [29]. The capacity of compensator s_{comp}^{-} is defined as:

$$S_{comp}^{-} = S_{u1} - S_{\Sigma}^{-} \tag{23}$$

where S_{Σ}^{-} is the negative sequence capacity that can make the VUF of bus x meet the VU limit pre-assessment, which can be defined as:

$$S_{\Sigma}^{-} = E_{x:j} S_{sc:x} \tag{24}$$

5.3 Optimal design

As shown in Fig. 7, HSR grid connection scheme optimization is advanced in this paper, considering traction characteristics and the power grid environment. Firstly, a uniform VU propagation model is built, and a NSP distribution area will be given. Secondly, the grid connection scheme will be designed to meet the suggestion above, and the VU limit for each TSS will be pre-assessed. Finally, the grid connection scheme is optimized, taking the accumulation capacity of the compensator as an object, as shown in Fig. 6.

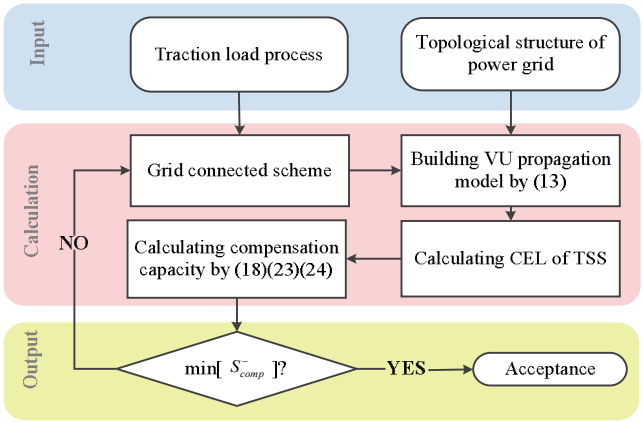

Fig. 7. *Flow chart of the design process*

6. Case study

6.1 Verification of the process

6.1.1 Test system description: In mid-western China, a vulnerable power grid structure and low short-circuit capacity are general characteristics of the power grid. A circle-wise power system with a single source is the typical power supply solution of a TPSS. As shown in Fig. 8, a three-bus test system (220 kV/50 Hz, three-phase) is established, assuming that the background VUF of the test system is aroused by two equivalent unbalanced constant power loads (L1 and L2), and the upstream system is symmetric. The background VUF is shown in Table 1, the influence coefficients of the test system are listed in Table 2, and other parameters of the test system are listed in *Appendix C*.

To verify the correctness of the model and the rationality of the pre-assessment process, the VU limit pre-assessment of the TSS and optimal design of the grid connection scheme are fully exhibited in this case study.

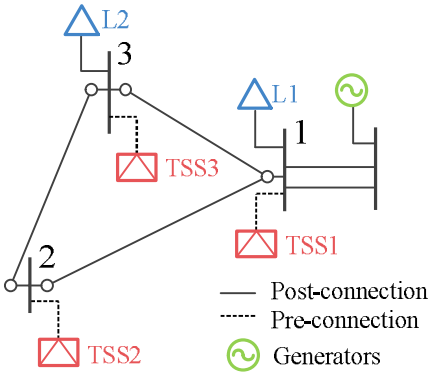

Fig. 8. *Three-bus test system*

Table 1 Background VUF

Bus number	VUF (%)	$\dot{U}_x^-$ (kV)
Bus 1	1.65	1.18∠19.88°
Bus 2	1.62	1.13∠12.71°
Bus 3	1.61	1.10∠5.05°

Table 2 Influence coefficients

$k_{i:x}$	Value	$k_{i:x}$	Value
k_{12}	0.4674	k_{31}	$-0.0266-0.0007j$
k_{21}	$0.2444+0.0058j$	k_{23}	$-0.6586+0.0004j$
k_{13}	$0.0653+0.0001j$	k_{32}	$0.5133+0.0004j$

To improve the authenticity of the case study, the data for the traction load is from the Beijing–Shanghai HSR, which can represent a typical feature of Chinese HSRs. Three TSSs of the Beijing–Shanghai HSR were measured in December 2017. The 95% probability values for current and voltage are shown in Table 3.

Table 3 Current and voltage of the feeding section

	TSS1	TSS2	TSS3
α feeding current (A)	658	696	642
β feeding current (A)	556	548	595
α feeding voltage (kV)	26.91	26.70	26.78
β feeding voltage (kV)	26.93	26.89	26.91

The average values of the power factor in 24 h are shown in Table 4. The power factor in most of the HSR TSSs is in range of 0.96 ~ 1, as the PWM converters are used in electric multiple units (EMUs).

Table 4 Power factor (PF) of the feeding section

	TSS1	TSS2	TSS3
α feeding PF	0.97	0.96	0.98
β feeding PF	0.96	0.98	0.97

The model consists of a background negative sequence voltage (NSV) vector when the test system is only connected to general unbalanced loads L1 and L2, and is shown in Fig. 9 by using the technique proposed by Sun *et al.* [13] and in section 3.

In Fig. 9(a), loads L1 (U_{L1}^-) is the main contributors for bus 1 (U_1^-), and bus 2 ($k_{2:1}U_2^-$) make a positive contribution to reduce the VUF at bus 1; in Fig. 9(b), The NSV at bus 2 (U_2^-) is the accumulated result from buses 1 ($k_{1:2}U_1^-$) and 3 ($k_{3:2}U_3^-$); in Fig. 9(c), load L2 (U_{L2}^-) is the main contributors for bus 3 (U_3^-), and bus 2 ($k_{2:3}U_2^-$) make a positive contribution to reduce the VUF at bus 3. Hence, to avoid degenerating the VUF of the power grid, the HSR grid connection scheme at bus 2 must be different from another bus. It should be noticed that the VU propagated between bus 1 and bus 3 (e.g. $k_{3:1}U_3^-$, $k_{1:3}U_1^-$) is very weak because the mutual implement is bigger than that of the other bus.

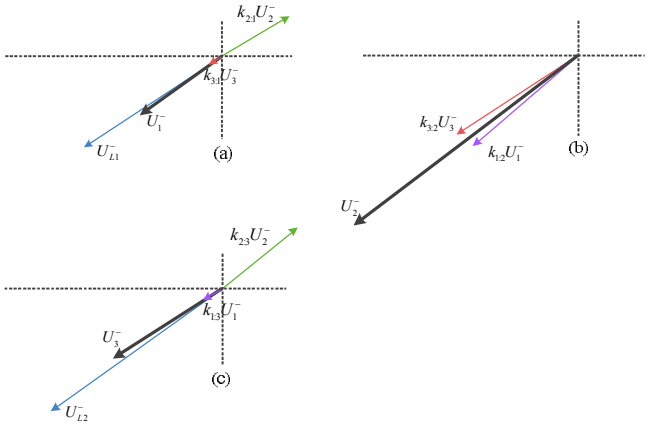

Fig. 9. *Resultant influence of the interaction of all unbalanced sources. (a) bus 1,(b) bus 2 and (c) bus 3 (drawn approximately to a scale)*

According to the discussion above, three reasonable grid connection schemes have been designed. As shown in Table 5, the traction transformer type for case 1 adopts the V/v transformer, which it is adopted wildly in Chinese HSRs; the Scott traction transformer has been used in Japan, Korea and etc, thus it is arranged to different position for case 2 and case 3.

Table 5 Grid connection scheme: traction transformer type

	TSS1	TSS2	TSS3
Case 1	V/v	V/v	V/v
Case 2	Scott	V/v	V/v
Case 3	V/v	V/v	Scott

The EPC scheme is shown in Table 6 and the values for the traction transformer phase angle is list in *Appendix A*. To reduce the quantity of electrical separation, the phase sequence for two adjacent feeding sections should stay in step.

Table 6 Grid connection scheme: EPC scheme

	TSS1	TSS2	TSS3
Case 1	CA/BA	BA/BC	BC/AC
Case 2	C/BA	BA/BC	BC/AC
Case 3	CA/BA	BA/BC	BC/A

6.1.2 VU limit pre-assessment: Fig. 10 shows the apparent power components of the TSS in each case; positive apparent power is similar in each case, and unbalanced apparent power is different for different grid connection schemes. This result reflects the relationship between apparent power and grid connection scheme; further, the correctness of the model established in sections 2 and 3 is verified.

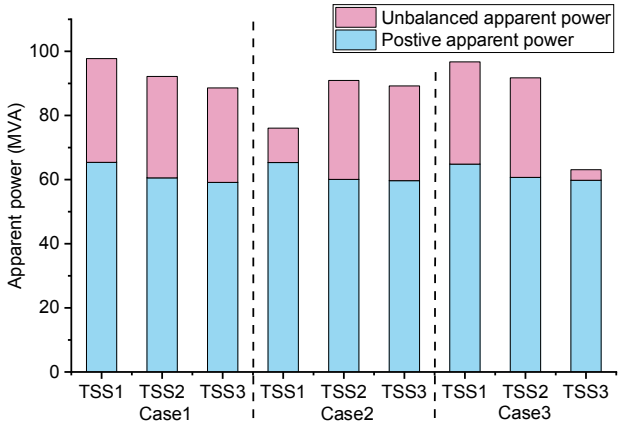

Fig. 10. *Components of apparent power*

And then, when the bus planning level ($U_{g:x}$) is set to 2%, the total available apparent power of the entire system ($S_{tot:x}$), the apparent power of customer ($S_{x:j}$), the allocated coefficient (k_a) and CELs ($E_{x:j}$) are calculated, and they are listed in Table 7. It can be easily found that the apparent power of customer installation larger, the CEL higher. For example, the CEL of TSS3 is larger than L2 in case 1, but in case3, the result is opposite, which means the pre-assessment process is based strictly on load capacity rather than on load type. On the other hand, the CELs for TSS2 in each case are different, although the grid connection schemes are same, it reflects that the CELs are not only related to the load capacity, but also related to the power grid environment.

Table 7 Calculation detail of CEL

	Bus x	$S_{tot:x}$ (MVA)	Load j	$S_{x:j}$ (MVA)	k_a	$E_{x:j}$ (%)
Case 1	1	179.45	TSS1	97.72	0.0449	1.18
			L1	68.27		0.92
	2	203.25	TSS2	92.17		1.13
	3	191.87	TSS3	88.59		1.11
			L2	50.56		0.74
Case 2	1	157.63	TSS1	76.06	0.0463	1.02
			L1	68.27		0.94
	2	194.78	TSS2	90.92		1.16
	3	191.33	TSS3	89.21		1.14
			L2	50.56		0.76
Case 3	1	178.23	TSS1	96.71	0.0467	1.22
			L1	68.27		0.95
	2	192.45	TSS2	91.74		1.18
	3	166.10	TSS3	63.08		0.90
			L2	50.56		0.77

Further, the allocated VU limit and simulated prospective VUF are compared in Fig. 11. As seen from Fig. 11, the prospective VUF for both cases 1 and 3 exceeds the allocated limit, thus there is a need to adopt some method to meet the limit. In case 2, the prospective VUF for TSS1 is lower than the VU limit, which means TSS1 passes the VU limit pre-assessment.

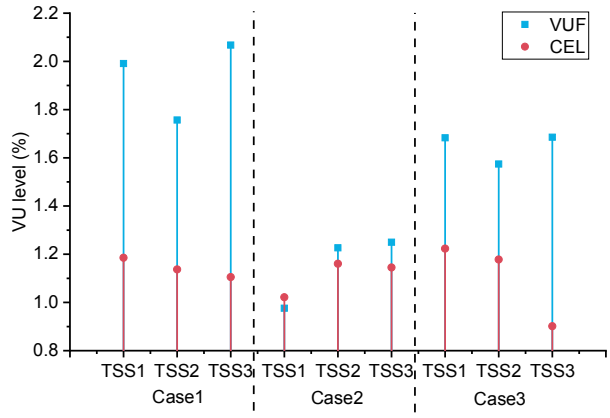

Fig. 11. *Results of pre-assessment*

Fig. 12 compares the background VUF and prospective VUF of the TSS, and conclusions drawn from it. (1) Comparing with the background VUF and case 2, for example, the background VUF of the bus1 is equal to 1.63%, however, it has been cut down to 0.97% in the case 2. A reasonably designed TPSS grid connection scheme can effectively reduce the impact on the power system. (2) Comparing the cases 1 and 2, such as the VUF of the bus 1 is 1.99% for case 1, and it is equal to 0.97% for case 2. Installing a V/v traction transformer for each TSS is not the best solution to lessen the VUF. (3) Comparing the cases 2 and 3, such as the VUF of the bus 3 is 1.25% for case 2, and it has arrival to 1.68% for case 3. Installing a reasonably balanced traction transformer such as a Scott transformer at a special bus can provide good performance and even reduce VUF.

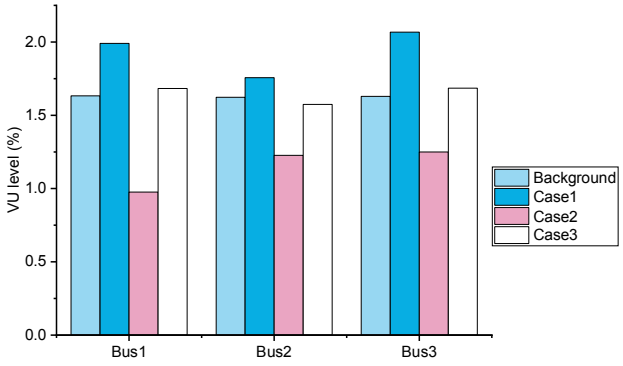

Fig. 12. *Compared results of background VUF and prospective VUF of a TSS*

6.1.3 HSR grid connection scheme optimization: Table 8 shows the unbalanced apparent power (S_{u1}), the capacity of compensator (S_{comp}^{-}) and the negative sequence capacity (S_{Σ}^{-})

for each case; the calculation process is given in Fig. 7. It can be found that the S_{comp}^{-} of TSS1 is zero in case2, this result keep consistent with Fig. 11. Therefore, the correctness of the improved VU limit pre-assessment process is verified via two different calculation methods.

Table 8 Computational details

	Load j	S_{u1} (MVA)	S_{Σ}^{-} (MVA)	S_{comp}^{-} (MVA)
Case 1	TSS1	32.32	23.71	8.61
	TSS2	31.65	22.73	8.91
	TSS3	29.46	22.10	7.36
Case 2	TSS1	10.73	20.43	0
	TSS2	30.86	23.21	7.64
	TSS3	29.56	22.90	6.66
Case 3	TSS1	31.87	24.47	7.41
	TSS2	31.06	23.56	7.50
	TSS3	3.27	18.03	0

The accumulated compensator capacity of the three TSSs is shown in Fig. 13. Case 2 is the best HSR grid connection scheme for this test system: not only is the sum of the capacity of the three TSSs minimized, but it could also lessen the excited VUF.

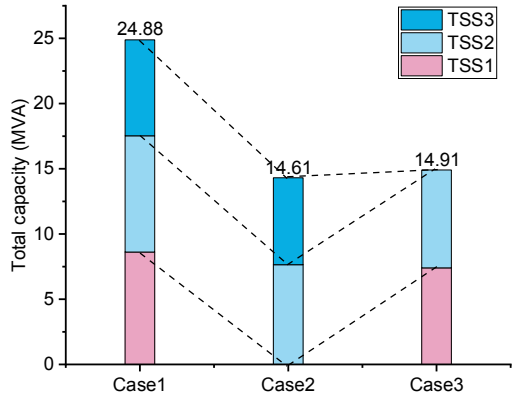

Fig. 13. *Accumulated compensator capacity of the three TSSs*

6.2 Uncertainty analysis for traction loads

The load uncertainty is also a major characteristic of traction load. Fig. 14 present the currents of α and β phases, and the maximal values for current and their corresponding voltage are shown in Table 9. The 95% probability values of the α phase is 658A, but the instantaneous current has arrived to 2663.6A, the wide current distributions is becoming an import factor that affects the VU distribution of power system. Therefore, the load uncertainty must be considered when implementing the VU limit pre-assessment.

Actually, the maximal values and 95% probability values are wildly used in power quality assessment, in which can portray the characteristic for load uncertainty. The power system operators have considered the load uncertainty when formulating the VU standards: the GB/T 15543 [18] set that the VUF of bus shall not exceed 4% between 3s and 60s during load power in a maximum state.

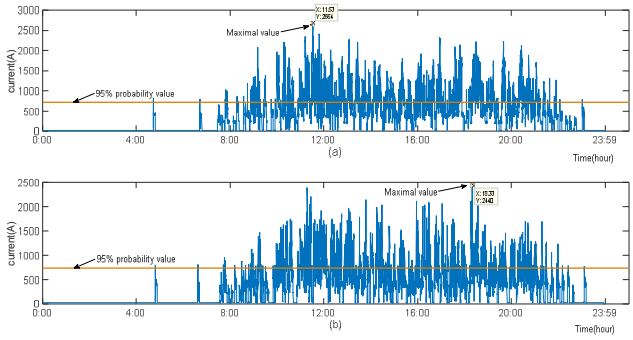

Fig. 14. *Currents of α and β phases during 24 h. (a) α phase and (b) β phase*

Table 9 Current and voltage of the feeding section

	TSS1	TSS2	TSS3
α feeding current (A)	2663.6	2683.7	2624.9
β feeding current (A)	2440.2	2613.4	2583.8
α feeding voltage (kV)	26.69	26.53	26.94
β feeding voltage (kV)	27.06	26.28	27.21

The test system is given in Fig. 8, adopting with the same calculation approach, and the bus planning level ($U_{g:x}$) is set to 4%. The apparent power of customer installation ($S_{x:j}$) and CEL ($E_{x:j}$) for each TSS is shown in Fig. 15, it can be easily find that the CELs are associated with the load capacity and network environment: the $S_{x:j}$ larger, the CEL higher, the TSS2 is also given to a different CEL value under the same grid connection scheme at same time. As a result, when traction load under the maximum traction condition, pre-assessment process is effective.

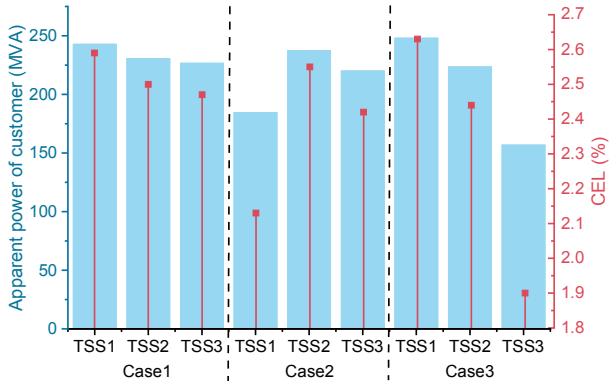

Fig. 15. Comparison of $S_{x:j}$ and $E_{x:j}$ for each TSS

Table 10 shows the accumulated compensator capacity of the three TSSs. The result is consistent with the section 6.1: Case 2 is the best HSR grid connection scheme for this test system.

Table 10 Accumulated compensator capacity

	Case1	Case 2	Case 3
Total capacity (MVA)	83.8	56.36	58.97

6.3 Analysis of IEEE 14-bus system

To verify the generality of the pre-assessment process, an IEEE 14-bus test system is established as shown in Fig. 16. The voltage level of test system is 220kV/50Hz (see *Appendix C)*, and the test system is assumed to supply three-phase symmetrical source and constant power load [10]; Three TSSs are connected to buses 2, 11 and 14, respectively, and the data for traction load is given in Tables 3 and 4.

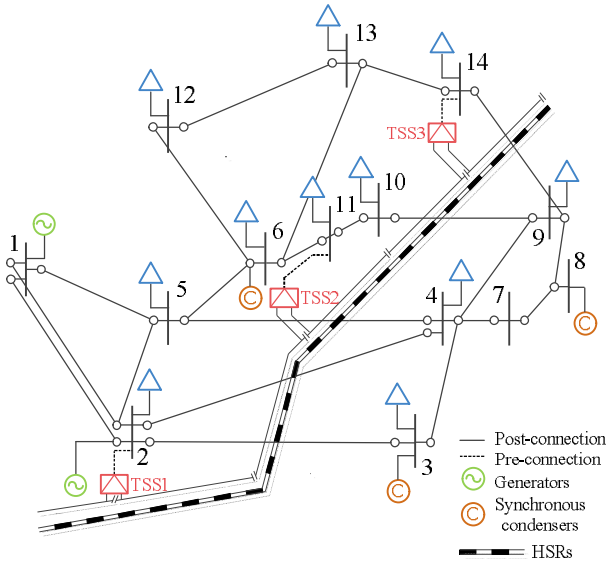

Fig. 16. *IEEE 14-bus test system*

Assuming all the traction transformer type adopt the V/v transformer, and the EPC scheme is shown in Table 11. The EPC technique is not used in the case 1, the number of EPC for the case 2 and case 3 are one, and the number of EPC for the case 4 is two, it means all the TSSs adopt the EPC technique.

Table 11 Grid connection scheme: EPC scheme

	TSS1	TSS2	TSS3	Num.
Case 1	CA/BA	CA/BA	CA/BA	0
Case 2	CA/BA	CA/BA	BA/BC	1
Case 3	CA/BA	BA/BC	BA/BC	1
Case 4	CA/BA	BA/BC	BC/AC	2

As shown in Fig. 17, comparison of case 1 and case 4, for example, the CEL for TSS3 is 1.26 and 1.19, respectively. It can be drawn a conclusion that the number of EPC influence the CEL when carrying out the pre-assessment process, meanwhile the VU pre-assessment process is valid when applying to a complex test system.

On the other way, a special phenomenon should be noted, take a TSS 3 as an example, although the number of EPC for the case 2 and case 3 are one, the VUF is distinct: the VUF for case 3 is approximate to case 1, and the case 2 is approximate to case 4. As a conclusion, comparison of case 1 and case 4, adopting the the EPC technique is effective that reduce the influence of TPSS on VUF for a power system; comparison of case 2 and case 4, the number of EPC has an apparent impact on VUF, it is interesting that discussing the number of EPC when optimize a grid connection scheme.

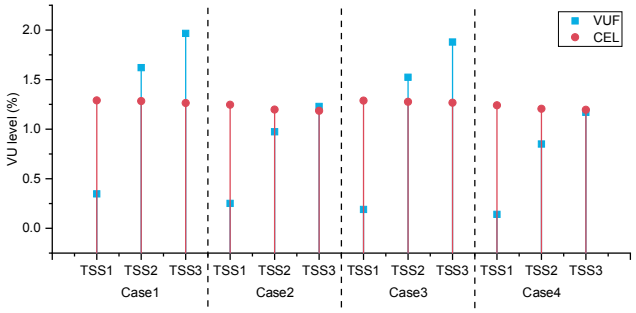

Fig. 17. *Results of pre-assessment.*

In order to illustrate above special phenomenon，based on a presented uniform VU propagation model in section 3, the model consists of a NSV vector is shown in Fig. 18.

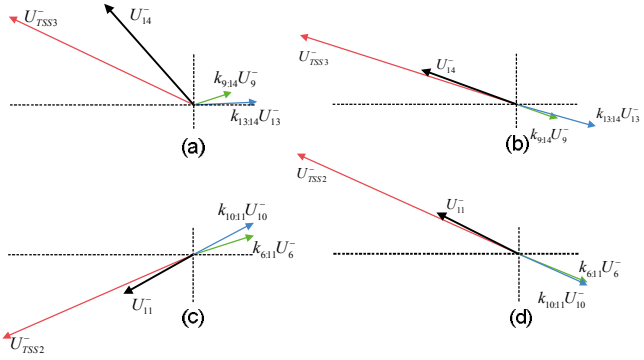

Fig. 18. *Resultant influence of the interaction of all unbalanced sources. (a) and (c) represents the case2, (b) and (d) represents the case 3 (drawn approximately to a scale)*

In Fig.18, the NSV vectors U_9^- and U_{13}^- are aroused mainly by TSS2, and U_6^- and U_{10}^- are aroused mainly by TSS3. In case 2, the varying NSV vectors offsets some part of impact on VUF, as shown in Fig. 17 (a) and (c); but the NSV vectors aggravates the impact on VUF in case 3, as shown in Fig. 17 (b) and (d).

7. Conclusion

In this paper, an improved VU limit pre-assessment process for HSR considering the grid connection scheme is proposed. The grid connection scheme is a vital part of TPSS design that obviously affects the VUF of power systems.

A uniform mathematical model of VU propagation considers the influence of the grid connection scheme that has been established, based on influence coefficients. This work reveals the impact of multiple grid connection schemes on the VU propagation behaviour of a three-phase grid. Subsequently, an improved VU limit pre-assessment process in terms of the grid connection scheme and power grid structure has been proposed; the relationship between grid connection scheme and VU limit has been established, at the same time meeting the requirements of IEC/TR 61000-3-13. Furthermore, summarizing the latest compensation technique for the TPSS, an unbalanced compensation calculation has been presented, and an optimal design for a grid connection scheme has been presented by minimizing accumulated compensator capacity as a target. Under the traction power in the maximal level and 95% probability level condition,

respectively, the correctness of the proposed VU limit pre-assessment process for HSR and the validity of the HSR grid connection scheme optimization process is verified. Furthermore, the generality of the proposed VU limit pre-assessment process is proved via an IEEE 14-bus test system.

For an actual railway system, the apparent power for each TSS cannot reach the maximum value at same time, as the high-speed train is dynamic. To fully use the ability of the system to regulate the VU level, it is worth discussing the simultaneity of maximum power between different TSSs in the future.

8. Acknowledgments

This work was supported by the National Natural Science Foundation of China (grant no. 51877182) and Science and Technology Projects of Sichuan Province (grant no. 2018FZ0107).

9. References

[1] Chen, M., Li, Q., Roberts, C. *et al.*: 'Modelling and performance analysis of advanced combined co-phase traction power supply system in electrified railway', *IET Gener. Transm. Dis.*, 2016, **10**, (4), pp. 906–916

[2] Serrano-Jiménez, D., Abrahamsson, L., Castaño-Solís, S., Sanz-Feito, J.: 'Electrical railway power supply systems: Current situation and future trends', *Int. J. Electric. Power*, 2017, **92**, pp. 181–192

[3] Stamatopoulos, A., Vikelgaard, H., Faria da Silva, F., Leth Bak, C.: 'Power system unbalance due to railway electrification: Review of challenges and outlook of the Danish case'. *Proc. IEEE Energy Conference, Leuven, Belgium, April 2016*, pp. 1–6

[4] Gazafrudi, S.M.M., Langerudy, A.T., Fuchs, E.F., Al-Haddad, K.: 'Power quality issues in railway electrification: A comprehensive perspective', *IEEE Trans. Ind. Elect.*, 2015, **62**, (5), pp. 3081–3090

[5] Hu, H., He, Z., Wang, K., Ma, X., Gao, S.: 'Power-quality impact assessment for high-speed railway associated with high-speed trains using train timetable—Part II: Verifications, estimations and applications', *IEEE Trans. Power Del.*, 2016, **31**, (4), pp. 1482-1492

[6] Wang, T., Nian, H., Zhu, Z. Q., Huang. *et al.*: 'Flexible PCC voltage unbalance compensation strategy for autonomous operation of parallel DFIGs', *IEEE Trans. Ind. Appl.*, 2017, **50**, (5), pp. 4807–4820

[7] Nian, H., Wang, T., Zhu, Z. Q.: 'Voltage imbalance compensation for doubly fed induction generator using direct resonant feedback regulator', *IEEE Trans Energy Conv.*, 2016, **31** (2), pp. 614-626

[8] China Electric Power Research Institute: 'Power quality testing and assessment of Datang Sanmenxia wind-farm' (China Electric Power Research Institute, 2009), pp. 1–56

[9] Ding, F., Zhang D., He, J., Liu, H., Li, Y.: 'Evaluation of the influence of electrified railway on wind farm', *Proc. IEEE Transportation Electrification Conference and Expo, Asia-Pacific, Harbin, China, Aug 2017,* pp. 1–6

[10] Jayatunga, U., Perera, S., Ciufo, P., Agalgaonkar, A.: 'Deterministic methodologies for the quantification of voltage unbalance propagation in radial and interconnected networks', *IET Gener. Transm. Dis.*, 2015, **9**, (11), pp. 1069–1076

[11] Jayatunga, U., Perera, S., Ciufo, P.: 'Voltage unbalance emission assessment in radial power systems', *IEEE Trans. Power Del.*, 2012, **27**, (3), pp. 1653–1661

[12] Jayatunga, U, Perera, S., Ciufo, P., Agalgaonkar, A.: 'Voltage unbalance emission assessment in interconnected power systems', *IEEE Trans. Power Del.*, 2013, **28**, (4), pp. 2383–2393

[13] Sun, Y., Li, P., Li, S., Xhang, L.: 'Contribution determination for multiple unbalanced sources at the point of common coupling', *Energies*, 2017, **10**, (171), pp. 1–17

[14] Mahyar, A., S, G, Seifossadat., M, Razaz., S, S, Moosapour.: 'Determining the contribution of different effective factors to individual voltage unbalance emission in n-bus radial power systems', *Int. J. Elect Power. Energy Syst.,* 2018, **94**, pp. 393–404

[15] Sun, Y., Xie, X, M., Peixin Li.: 'Unbalanced source identification at the point of evaluation in the distribution power systems', *Int. Trans. Electric. Energy Syst.,* 2018, **28**. (1), pp. 1–20

[16] Wen, He., Cheng, D., Teng, Z. *et al.*: 'Approximate algorithm for fast calculating voltage unbalance factor of three-phase power system', *IEEE Trans. Ind. Inf.,* 2014, **10**. (3), pp. 1799–1805

[17] Perera, D., Ciufo, P., Meegahapola, L., Perera, S.: 'Attenuation and propagation of voltage unbalance in radial distribution networks', *Int. T. Electr. Energy*, 2015, **25**, (12), pp. 3738–3752

[18] China National Standardization Management Committee: 'GB/T 15543-2008: Power quality: Three-phase voltage unbalance' (General Administration of Quality Supervision, Inspection and Quarantine (GAQSIQ); Standardization Administration (SAC) of the People's Republic of China, 2008)

[19] International Electrotechnical Commission: 'IEC/TR 61000-3-13: Electromagnetic compatibility (EMC) – limits – assessment of emission limits for the connection of unbalanced installations to MV, HV and EHV power systems' (International Electrotechnical Commission, 2008)

[20] Paranavithana, P., Perera, S., Koch, R.: 'A generalised methodology for evaluating voltage unbalance influence coefficients'. *Proc. 20th Int. Conf. and Exhibition on Electricity Distribution – Part 1, Prague, Czech Republic, June 2009*, pp. 1–4

[21] Paranavithana, P.: 'Contributions towards the development of the technical report IEC/TR 61000-3-13 on voltage unbalance emission allocation', PhD thesis, University of Wollongong, 2009

[22] Jayatunga, U., Perera, S., Ciufo, P., Agalgaonkar, A, P.:' A refined general summation law for VU emission assessment in radial networks', *Electr Power Energy Syst.*, 2015, **73**, pp. 329–39

[23] National Grid Electricity Transmission: 'The grid code, issue 5, revision 21' (National Grid Electricity Transmission, 2017)

[24] Standards Australia: 'AS/NZS 61000-3-13 - Electromagnetic compatibility (EMC) - Part 3.13 Limits - Assessment of emission limits for the connection of unbalanced installations to MV, HV and EHV power systems' (Standards Australia, 2012)

[25] Energinet.dk: 'Teknisk forskrift 3.4.1 – Spændindgs-kvalitet' (Energinet, 2013)
[26] Paranavithana, P., Perera, S.: 'A robust voltage unbalance allocation methodology based on the IEC/TR 61000-3-13 guidelines'. *Proc. IEEE Power Engineering Society General Meeting, Calgary, Alberta, Canada, July 2009*, pp. 1–6
[27] Emanuel, A.E.: 'Summary of IEEE standard 1459: Definitions for the measurement of electric power quantities under sinusoidal, non-sinusoidal, balanced, or unbalanced conditions', *IEEE Trans. Ind. Appl.*, 2004, **40**, (3), pp. 869–876
[28] Kukačka, L., Kraus, J., Kolář, M., Dupuis, P., Zissis, G. .: 'Review of AC power theories under stationary and non-stationary, clean and distorted conditions', *IET Gener. Transm. Dis.*, 2016, **10**, (1), pp. 221–231
[29] IEEE: 'IEEE standard definitions for the measurement of electric power quantities under sinusoidal, nonsinusoidal, balanced, or unbalanced conditions' (IEEE, 2010) *(Revision of IEEE Std 1459-2000)*
[30] Tshepo, S., Rens, J.: 'Practical evaluation of voltage unbalance at a distribution transformer based on 50 Hz negative sequence active power'. *Proc. of AFRICON, Livingstone, Zambia, November 2011*, pp. 1–4
[31] Roudsari, H, M., Jalilian, A., & Jamali, S.: 'Flexible Fractional Compensating Mode for Railway Static Power Conditioner in V/v Traction Power Supply System', *IEEE Trans. Ind. Elect.*, 2018, **65**, (10), pp. 7963–7974
[32] Xu, Q., Ma, F., He, Z., Chen, Y., Guerrero, J. M., Luo, A., Yue, Y.: 'Analysis and comparison of modular railway power conditioner for high-speed railway traction system', *IEEE Trans. Power Electron.*, 2017, **32**, (8), pp. 6031–6048
[33] Li, Q.: 'New generation traction power supply system and its key technologies for electrified railways', *J Mod Transp.*, 2015, **23**, (1), pp. 1–11
[34] He, X., Guo, A., Peng, X., Zhou, Y., Shi, Z., Shu, Z.: 'A traction three-phase to single-phase cascade converter substation in an advanced traction power supply system', *Energies.*, 2015, **8**, (9), pp. 9915–9929
[35] Dai, N, Y., Lao, K, W., Lam, C. S.: 'Hybrid railway power conditioner with partial compensation for rating optimization', *IEEE Trans. Ind. Appl.*, 2015, **51**, (5), pp. 4130–4138
[36] Dai, N, Y., Wong, M, C., Lao, K, W., Wong, C, K.: 'Modelling and control of a railway power conditioner in co-phase traction power system under partial compensation', *IET Power Elect.*, 2014, **7**, (5), pp. 1044–1054

10. Appendices

Appendix A

For the V/v traction transformer, $\Psi_\beta = \Psi_\alpha + 120°, K_\alpha = K_\beta = k_T$, the current transformation matrix M and voltage transformation matrix N is shown as:

$$V = C^T = k_T \begin{bmatrix} 2\cos\psi_\alpha & 2\cos\left(120^\circ + \psi_\alpha\right) \\ 2\cos\left(120^\circ - \psi_\alpha\right) & 2\cos\psi_\alpha \\ 2\cos\left(120^\circ + \psi_\alpha\right) & 2\cos\left(120^\circ - \psi_\alpha\right) \end{bmatrix} \quad (26)$$

The inverse matrix is shown as:

$$V^{-1} = \left(C^{-1}\right)^T = \frac{1}{3k_T} \begin{bmatrix} 2\sin\left(120^\circ + \psi_\alpha\right) & -2\sin\psi_\alpha \\ 2\sin\psi_\alpha & 2\sin\left(120^\circ - \psi_\alpha\right) \\ -2\sin\left(120^\circ - \psi_\alpha\right) & -2\sin\left(120^\circ + \psi_\alpha\right) \end{bmatrix}^T \quad (27)$$

For the Scott traction transformer, $\Psi_\beta = \Psi_\alpha \pm 90°, K_\alpha = K_\beta = k_T$, the current transformation matrix M and voltage transformation matrix N is shown as:

$$V = C^T = k_T \begin{bmatrix} 2\cos\psi_\alpha & -2\sin\psi_\alpha \\ 2\cos\left(120^\circ - \psi_\alpha\right) & 2\sin\left(120^\circ - \psi_\alpha\right) \\ 2\cos\left(120^\circ + \psi_\alpha\right) & -2\sin\left(120^\circ + \psi_\alpha\right) \end{bmatrix} \quad (28)$$

The inverse matrix is shown as:

$$V^{-1} = \left(C^{-1}\right)^T = \frac{1}{3k_T} \begin{bmatrix} 2\cos\psi_\alpha & 2\sin\psi_\alpha \\ 2\cos\left(120^\circ - \psi_\alpha\right) & 2\sin\left(120^\circ - \psi_\alpha\right) \\ 2\cos\left(120^\circ + \psi_\alpha\right) & -2\sin\left(120^\circ + \psi_\alpha\right) \end{bmatrix}^T \quad (29)$$

Table 12 gives the values for the traction transformer phase angle.

Table 12

ψ_α	Value	ψ_α	Value
ψ_A	0°	ψ_{CB}	90°
ψ_B	−120°	ψ_{BC}	270°
ψ_C	120°	ψ_{AC}	330°
ψ_{AB}	30°	ψ_{CA}	150°
ψ_{BA}	210°		

Appendix B

● *Port transformation matrix*

The equation (1) can be expressed as:

$$U^+_{abc} \begin{pmatrix} 1 & 1 & 1 \\ 1 & a^2 & a \\ 1 & a & a^2 \end{pmatrix} \dot{I}^*_{abc} = \begin{pmatrix} 0 \\ \sqrt{3}k_T \sum_{i=1}^{2} U^+_{abc} e^{-j\psi_i} \dot{I}^*_i \\ \sqrt{3}k_T \sum_{i=1}^{2} U^+_{abc} e^{j\psi_i} \dot{I}^*_i \end{pmatrix} \quad (25)$$

Thus, the relationship of the current on the grid and traction sides is expressed as (3).

● *Equivalent model of a TSS*

The relationship between the grid side and traction side current of a traction transformer is given in equation (26):

$$\dot{I}_{abc} = C\dot{I}_{\alpha\beta} \quad (26)$$

where $\dot{I}_{\alpha\beta}$ is the current matrix for the feeding section, which can be expressed as:

$$\dot{I}_{\alpha\beta} = \begin{bmatrix} \dot{I}_\alpha \\ \dot{I}_\beta \end{bmatrix} = \begin{bmatrix} I_\alpha \\ I_\beta \end{bmatrix}^{\mathrm{T}} \begin{bmatrix} e^{j(\psi_\alpha + \varphi_\alpha)} \\ e^{j(\psi_\beta + \varphi_\beta)} \end{bmatrix} \quad (27)$$

where φ_α and φ_β are the power factors of α and β feeding sections, respectively.

The relationship between the grid side and traction side voltage of a traction transformer is given in equation (28):

$$\dot{E}_{abc} = V^{-1}\dot{E}_{\alpha\beta} \tag{28}$$

Alternatively, the voltage matrix of the feeding section $\dot{U}_{\alpha\beta}$ can be expressed as:

$$\dot{U}_{\alpha\beta} = \begin{bmatrix} \dot{U}_{\alpha} \\ \dot{U}_{\beta} \end{bmatrix} = \begin{bmatrix} U_{\alpha} \\ U_{\beta} \end{bmatrix}^{\mathrm{T}} \begin{bmatrix} e^{j\varphi_{\alpha}} \\ e^{j\varphi_{\beta}} \end{bmatrix} \tag{29}$$

Appendix C

- *3-bus test system*

Table 13gives the basic parameters for the upstream system.

Table 13

$\dot{U}_{up-sys}$ (kV)	f (Hz)	S_{dc} (MVA)
$220 \angle 0°$	50	2000

Table 14 gives the approximate line lengths of test system.

Table 14

From bus	To bus	Approximate length of the line (km)
1	2	20
1	3	20
2	3	53

Table 15 gives the three-phase active and reactive power for each general load at the bus.

Table 15

	P_a (MW)	P_b (MW)	P_c (MW)	$Q_a = Q_b = Q_c$ (MVar)
L1	18.3	1	22.3	2.37
L2	15.3	15.3	2.38	5

The impedance matrix of the transposed line (Ω/km):

$$\begin{pmatrix} 0.2192 + j0.7313 & 0.04622 + j0.3317 & 0.04622 + j0.2882 \\ 0.04622 + j0.3317 & 0.2192 + j0.7313 & 0.04622 + j0.3317 \\ 0.04622 + j0.2882 & 0.04622 + j0.3317 & 0.2192 + j0.7313 \end{pmatrix}$$

- *IEEE 14-bus test system*

The impedance matrix of the transposed line (Ω/km):

$$\begin{pmatrix} 0.2952 + j0.7423 & 0.04622 + j0.2882 & 0.04620 + j0.2448 \\ 0.04622 + j0.2882 & 0.2952 + j0.7423 & 0.04622 + j0.2882 \\ 0.04620 + j0.2448 & 0.04622 + j0.2882 & 0.2952 + j0.7423 \end{pmatrix}$$